

# Infrared broadband nonlinear optical limiting technology based on stimulated Brillouin scattering in $\text{As}_2\text{Se}_3$ fiber

Jian Huang (黄剑)<sup>1,2</sup>, Yuangang Lu (路元刚)<sup>1,2\*</sup>, Zhengnan Wu (吴政南)<sup>1,2</sup>, Youwen Xie (谢有文)<sup>1,2</sup>, Chongjun He (赫崇君)<sup>1</sup>, and Junfeng Wu (武俊峰)<sup>1</sup>

<sup>1</sup>Key Laboratory of Space Photoelectric Detection and Perception of Ministry of Industry and Information Technology, College of Astronautics, Nanjing University of Aeronautics and Astronautics, Nanjing 210016, China

<sup>2</sup>College of Science, Nanjing University of Aeronautics and Astronautics, Nanjing 211106, China

\*Corresponding author: [luyg@nuaa.edu.cn](mailto:luyg@nuaa.edu.cn)

Received December 16, 2021 | Accepted December 29, 2021 | Posted Online January 24, 2022

A novel infrared broadband nonlinear optical limiting (NOL) technology based on stimulated Brillouin scattering (SBS) in  $\text{As}_2\text{Se}_3$  fiber is proposed. The  $\text{As}_2\text{Se}_3$  fiber allows a weak infrared laser to pass through, but blocks an intense laser with the same wavelength due to the SBS effect. This NOL technology has been experimentally proved to have excellent NOL performance for incident pulsed lasers with a typical infrared wavelength of 3.6  $\mu\text{m}$ . The linear transmissions of 1 m and 0.5 m  $\text{As}_2\text{Se}_3$  fibers are higher than 90%, and the lowest nonlinear transmissions are reduced to 0.89% and 1.23%, respectively.

**Keywords:** nonlinear optical limiting; stimulated Brillouin scattering;  $\text{As}_2\text{Se}_3$  fiber.

**DOI:** [10.3788/COL202220.031902](https://doi.org/10.3788/COL202220.031902)

## 1. Introduction

Nonlinear optical limiting (NOL) technology is to allow weak light to pass through with high transmission while blocking strong light with low transmission and thus can prevent the human eyes and sensitive optical sensors from being irreversibly damaged by high-intensity lasers<sup>[1]</sup>. In many cases, the studies of NOL performances are mainly focused on visible light to near-infrared laser radiation<sup>[2–4]</sup>, especially 532 nm and 1064 nm, and there are relatively few studies on the longer wavelengths. However, with the development of infrared high-power laser technology, high-power lasers have important applications in many fields, such as material processing<sup>[5]</sup>, biomedicine<sup>[6]</sup>, remote sensing<sup>[7]</sup>, and molecular spectroscopy<sup>[8]</sup>. In order to prevent human eyes and some sensitive sensors from high-power infrared lasers, it is necessary to explore NOL technology used in the infrared wavelength range. The main approaches of infrared broadband NOL technology are based on nonlinear absorption (NA)<sup>[9]</sup>, reverse saturable absorption (RSA)<sup>[10]</sup>, two-photon absorption (TPA)<sup>[11]</sup>, and phase change<sup>[12]</sup>. While it is relatively easy to protect against a single wavelength laser, the currently available broadband high-power laser sources require an NOL technology to operate in a wide wavelength range<sup>[13]</sup>. Therefore, it is greatly significant to study the infrared broadband NOL technology.

In this Letter, we innovatively propose an infrared broadband NOL technology based on stimulated Brillouin scattering (SBS) in  $\text{As}_2\text{Se}_3$  fiber. The  $\text{As}_2\text{Se}_3$  fibers have low-loss from 3 to 8  $\mu\text{m}$

(except for 4.5–4.8  $\mu\text{m}$ ), which ensures high transmission under weak light in a wide range of wavelengths<sup>[14]</sup>. When the intensity of the incident laser exceeds a certain limit, SBS occurs, and most of the incident laser will be scattered in the backward direction<sup>[15]</sup>. The SBS media achieve the purpose of NOL by back-scattering the strong incident laser instead of absorbing it, which effectively prevents the media from being damaged due to absorbing a large amount of energy<sup>[16]</sup>. Besides, optical fibers can provide long interaction length and localize the incident laser in the fiber core<sup>[17]</sup>, which is beneficial to exciting the SBS effect and improving the NOL performance. We experimentally verified that the 1 m and 0.5 m  $\text{As}_2\text{Se}_3$  fibers have excellent NOL performance for nanosecond pulsed laser with a typical infrared wavelength of 3.6  $\mu\text{m}$ . The linear transmissions of 1 m and 0.5 m  $\text{As}_2\text{Se}_3$  fibers are higher than 90%, and the lowest nonlinear transmissions are reduced to 0.89% and 1.23%, respectively. To the best of our knowledge, this is the first time to use  $\text{As}_2\text{Se}_3$  fiber as NOL media in the infrared wavelength range. The novel NOL media feature light weight, small size, and being easy to bend, which may easily achieve excellent NOL performance within a small volume. This NOL technology may have potential applications in all-optical communications<sup>[18]</sup>, sensor protection<sup>[19]</sup>, and other infrared broadband laser protection fields.

## 2. Principle

As is similar in other types of optical fibers, the SBS in  $\text{As}_2\text{Se}_3$  fiber is a nonlinear optical phenomenon caused by the

interaction of optical and acoustic waves in the optical fiber<sup>[20]</sup>. When the incident laser is weak, the laser transmits the fiber with the power losses generated from material absorption and Rayleigh scattering of the fiber. As the intensity of the incident laser gradually increases beyond the stimulated threshold to excite the SBS effect in the fiber, the energy of the forward transmitted laser will be transferred to the Stokes wave, which transmits backward. The dynamic process of the SBS can be modeled with the following equations<sup>[21]</sup>:

$$\begin{cases} \frac{\partial E_l(z,t)}{\partial z} + \frac{n}{c} \frac{\partial E_l(z,t)}{\partial t} = -\alpha E_l(z,t) + i\kappa\rho(z,t)E_s(z,t), \\ \frac{\partial E_s(z,t)}{\partial z} - \frac{n}{c} \frac{\partial E_s(z,t)}{\partial t} = -\alpha E_s(z,t) + i\kappa\rho^*(z,t)E_l(z,t), \\ \frac{\partial \rho(z,t)}{\partial t} + \frac{\Gamma}{2}\rho(z,t) = i\Lambda E_l(z,t)E_s^*(z,t) + f(z,t), \end{cases} \quad (1)$$

where  $E_l(z,t)$  and  $E_s(z,t)$  are, respectively, the pump and Stokes field amplitudes at time  $t$  and location  $z$ ,  $n$  is the refractive index,  $c$  is the speed of light,  $\rho(z,t)$  is the density,  $\alpha$  is the loss coefficient,  $\Gamma$  is the phonon decay rate,  $\kappa$  and  $\Lambda$  are Brillouin coupling constants, and  $f(z,t)$  is the thermal fluctuations in the density of the medium. By solving the transient solution of the coupled wave equation, the transmitted waveform related with SBS effect can be simulated under different incident power densities. The SBS threshold  $I_{th}$  is defined as the value of the power density when the Brillouin reflectivity reaches 0.01, which can be calculated by the following formula<sup>[22]</sup>:

$$I_{th} = \frac{G_{th}}{g_B L_{eff}}, \quad (2)$$

where  $G_{th}$  is the stimulated threshold parameter related to the optical fiber material,  $g_B$  is the Brillouin gain coefficient of optical fiber,

$$L_{eff} = \frac{1 - e^{-\alpha L}}{\alpha} \quad (3)$$

is the effective interaction length, and  $L$  is the length of optical fiber. The ratio of the backscattered and incident laser intensity is the SBS reflectivity  $R$ , which has the following relationship with the Brillouin gain coefficient  $g_B$  and the effective interaction length  $L_{eff}$ <sup>[21]</sup>:

$$g_B I L_{eff} = \frac{\ln R + G_{th}}{1 - R}. \quad (4)$$

In Eq. (4),  $I$  is the incident laser intensity defined as  $I = P/A_{eff}$ , where  $P$  is laser power,

$$A_{eff} = \frac{\left( \iint |F(x,y)|^2 dx dy \right)^2}{\iint |F(x,y)|^4 dx dy} \quad (5)$$

is the effective mode field area of the optical wave, and  $F(x,y)$  is the optical field distribution of the laser transmitted in the fiber<sup>[23]</sup>. The transmission of the optical fiber can be approximately expressed as  $T = 1 - A - R_s$ , where  $A$  is the absorption,

and  $R_s$  is the reflectivity, without considering fiber end face reflection due to refractive index mismatch. The reflectivity  $R_s$  includes SBS and Rayleigh scattering within the fiber. When SBS occurs, the intensity of Rayleigh scattering compared to SBS can be ignored, and  $R_s$  can be approximately equal to  $R$ . Therefore, Eq. (4) can be rewritten as

$$I = \frac{\ln(1 - A - T) + G_{th}}{g_B L_{eff}(A + T)}. \quad (6)$$

For applications involving SBS, it is hoped that the medium has large Brillouin gain coefficient  $g_B$  and long effective interaction length  $L_{eff}$  to stimulate the SBS effect easily, which can be clearly seen from Eq. (6). Therefore, in this Letter, the  $As_2Se_3$  fibers are selected as NOL media due to not only providing a long effective interaction length  $L_{eff}$ , but also a high Brillouin gain coefficient  $g_B$ , which is reported to be  $(6.75 \pm 0.35) \times 10^{-9} \text{ m/W}$ <sup>[24]</sup>. Besides, the laser induced damage threshold of  $As_2Se_3$  glass is as high as  $13 \text{ GW/cm}^2$ <sup>[25]</sup>, which is higher than that of most NOL materials. In addition, the  $As_2Se_3$  fibers have low average fiber loss (less than  $0.5 \text{ dB/m}$ ) in the range from  $3 \mu\text{m}$  to  $8 \mu\text{m}$  (except  $4.5\text{--}4.8 \mu\text{m}$ ), which can be used as an ideal broadband optical limiter.

### 3. Experimental Setup

The experimental setup used to evaluate the NOL performance of  $As_2Se_3$  fibers is shown in Fig. 1. A solid-state pulsed laser with a wavelength of  $3.6 \mu\text{m}$  was used as the light source for the experiment. The pulse frequency and pulse width of the laser were set to 1 Hz and 10 ns, respectively. An aperture with a diameter of 1 mm was added to ensure that the output laser is the fundamental mode. Two neutral density filters were used to prevent the energy meter and the photodetector from being damaged by the laser, respectively. The laser beam is divided into two beams by the beam splitter, and the energy meter was used to record the pulse energy of the laser. The fiber port was fixed on a three-dimensional (3D) translation stage in order to couple the laser into the fiber as much as possible. The fiber used in our experiment was commercial  $As_2Se_3$  fiber (IRflex Corporation)

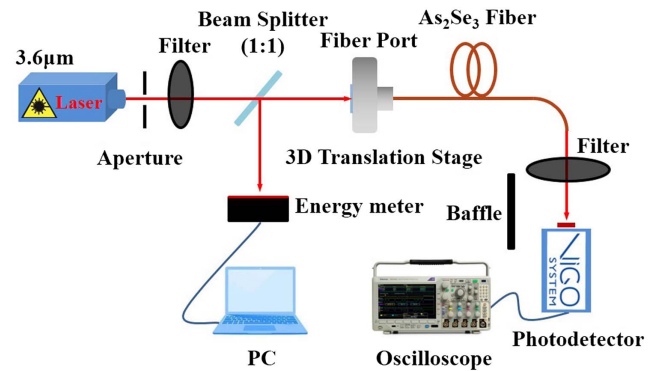


Fig. 1. Schematic diagram of the experimental setup.

with a core diameter and cladding diameter of 100  $\mu\text{m}$  and 170  $\mu\text{m}$ , respectively. According to Eq. (5), combined with the finite element analysis method, the average effective mode area  $A_{\text{eff}}$  is calculated to be 4032  $\mu\text{m}^2$ . We evaluated the NOL performance of  $\text{As}_2\text{Se}_3$  fibers with lengths of 1 m and 0.5 m, respectively. The intensity of the transmitted laser was detected by a photodetector, and the transmitted pulse was displayed on an oscilloscope. During the experiment, we set the laser current to control the intensity of the output laser. In each measurement, 20 data points were recorded and averaged to reduce measurement uncertainty.

#### 4. Results and Discussion

The NOL experimental results of 1 m and 0.5 m  $\text{As}_2\text{Se}_3$  fibers are shown in Fig. 2. The result of the output optical power density increasing with the incident optical power density is shown in Fig. 2(a). It can be seen from the Fig. 2(a) that the output power density increases linearly with the increase of the incident power density when the incident laser is weak. When the incident optical power densities exceed the SBS threshold, which are, respectively, 11.5  $\text{MW}/\text{cm}^2$  and 15.1  $\text{MW}/\text{cm}^2$  for 1 m and 0.5 m  $\text{As}_2\text{Se}_3$  fibers, the output power density increases more and

more slowly until there is no significant change. Finally, the output power density of the  $\text{As}_2\text{Se}_3$  fibers with lengths of 1 m and 0.5 m is stable around 12  $\text{MW}/\text{cm}^2$  and 16  $\text{MW}/\text{cm}^2$ , respectively, which shows a characteristic that an ideal NOL technology should possess<sup>[4]</sup>.

As shown in Fig. 2(b), when the incident laser is weak, the transmission remains high and almost unchanged so that the weak signal light can be transmitted with the light power loss of 4.8 dB/m at the wavelength of 3.6  $\mu\text{m}$ . However, the transmission decreases rapidly with increasing incident power density and eventually drops to 0.89% and 1.23% at the lowest level, respectively. The limiting threshold is defined as the incident power density where the transmission falls to 50% of the normalized linear transmission<sup>[26]</sup>. The limiting thresholds of the  $\text{As}_2\text{Se}_3$  fibers with lengths of 1 m and 0.5 m are 22.7  $\text{MW}/\text{cm}^2$  and 28.4  $\text{MW}/\text{cm}^2$ , respectively. For the laser with an incident wavelength of 3.6  $\mu\text{m}$  in our experiment, the incident photon energy  $\hbar\omega$  is smaller than  $E_g/2$ , which means that the TPA effect in the fiber will not be allowed at this wavelength<sup>[27]</sup>. Therefore, the absorption  $A$  in Eq. (6) of the  $\text{As}_2\text{Se}_3$  fiber can be approximately regarded as 0.48 dB/m at 3.6  $\mu\text{m}$ . By normalizing the transmission, we fit the experimental results with Eq. (6) and obtain the Brillouin gain coefficient  $g_B$  of  $\text{As}_2\text{Se}_3$  fiber to be  $6.70 \times 10^{-9}$  m/W, which is close to the previously reported results<sup>[28,29]</sup>. The results show that the NOL technology based on SBS in  $\text{As}_2\text{Se}_3$  fiber has excellent limiting performance for the infrared pulsed laser with a typical wavelength of 3.6  $\mu\text{m}$ . Moreover, the fiber we selected has high linear transmission in the infrared band (3–8  $\mu\text{m}$ ), where the average loss is less than 0.5 dB/m, except in the range from 4.5  $\mu\text{m}$  to 4.8  $\mu\text{m}$ , which ensures that the linear transmissions of the 1 m and 0.5 m  $\text{As}_2\text{Se}_3$  fibers can be higher than 90%. Since the SBS effect is independent of the wavelength of the incident laser, the NOL technology we proposed can respond to the intensity of the incident laser and realize the excellent NOL of the infrared broadband.

As shown in Fig. 3, the output pulses of the 1 m  $\text{As}_2\text{Se}_3$  fiber under different incident power densities can be clearly observed on the oscilloscope after the output pulses are detected by the photodetector. As illustrated in Fig. 3(a), the transmitted laser intensity increases linearly when the incident power density is too weak to excite the SBS effect, and thus the shape of the transmitted pulse is similar to that of the incident pulse. As the incident power density continues to increase beyond the SBS threshold (11.5  $\text{MW}/\text{cm}^2$ ), the incident laser beam will be scattered backward as the result of stimulated scattering processes. Therefore, the back edge of the transmitted pulse starts to drop abruptly, and the tail of pulse forms a “platform”<sup>[30]</sup>, which can be clearly observed in Fig. 3(b). The reason is that the intensity of the incident laser is above the SBS threshold, and the interaction between optical and acoustic waves is strong, which leads to a large amount of energy transfer to the Stokes wave propagating backward. The intensity of the backward Stokes wave increases, causing the tail of the transmitted pulse to drop sharply below the SBS threshold, so the intensity of the pulse tail maintains near the platform. Since the phonon lifetime of  $\text{As}_2\text{Se}_3$  is about

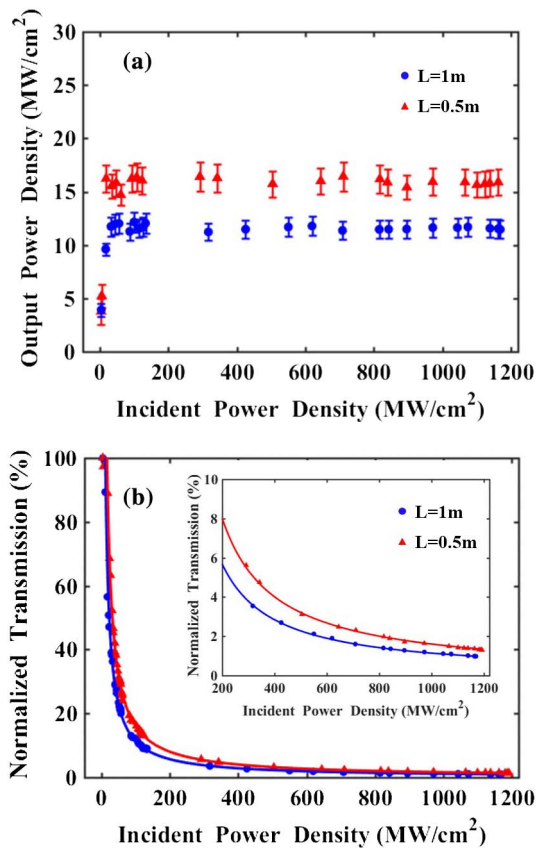
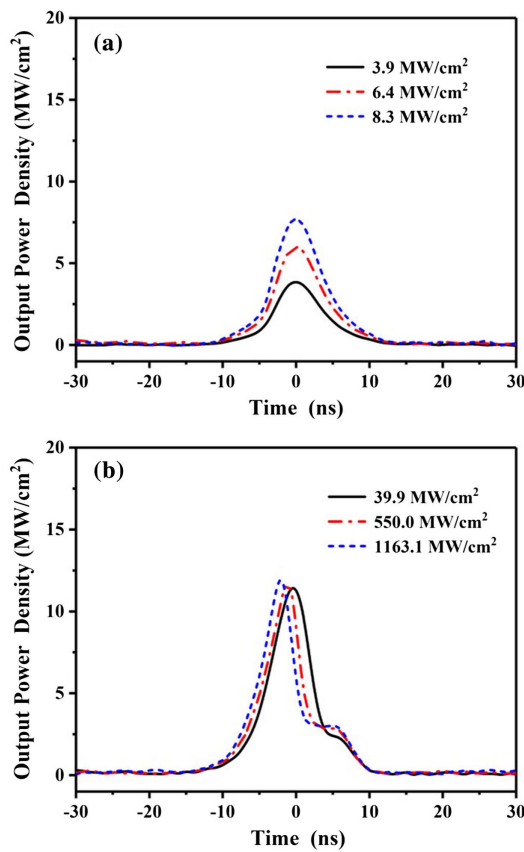


Fig. 2. NOL experimental results of  $\text{As}_2\text{Se}_3$  fibers with the length of 1 m and 0.5 m. (a) Output power density increases with the incident power density. (b) Normalized transmission decreases with the incident intensity.



**Fig. 3.** Transmitted pulses under low and high incident power densities. (a) Transmitted pulses with the low incident intensity of 3.9 MW/cm<sup>2</sup>, 6.4 MW/cm<sup>2</sup>, and 8.3 MW/cm<sup>2</sup>, respectively. (b) Transmitted pulses after the SBS effect occurs with the high incident intensity of 39.9 MW/cm<sup>2</sup>, 550.0 MW/cm<sup>2</sup>, and 1163.1 MW/cm<sup>2</sup>, respectively.

1 ns<sup>[31]</sup>, the entire NOL process can be completed within a few nanoseconds, which indicates that this NOL technology can easily and quickly deal with the intense hostile or accidental lasers.

As shown in Table 1, we list some NOL performances of 1 m and 0.5 m As<sub>2</sub>Se<sub>3</sub> fibers and compare several infrared broadband NOL technologies based on other principles in recent years<sup>[10,12,32]</sup>. In contrast, the NOL technology we proposed

in this Letter has the advantages of excellent NOL performance, high laser induced damage threshold, and wide applicable wavelength range.

## 5. Conclusion

In summary, we propose an infrared broadband NOL technology based on the SBS effect in As<sub>2</sub>Se<sub>3</sub> fiber. The experimental results show that this NOL technology has excellent limiting performance for a pulsed laser with a typical infrared wavelength of 3.6 μm. The linear transmissions of 1 m and 0.5 m As<sub>2</sub>Se<sub>3</sub> fibers are higher than 90%, and the lowest nonlinear transmissions are reduced to 0.89% and 1.23%, respectively. The advantage of SBS-based NOL is that most of the energy is transferred to backscattering instead of absorption, avoiding thermal effects on the material and thus avoiding the bad effect on NOL performance. In addition, the SBS-based technology has broadband excellent NOL performance because SBS is not sensitive to wavelength. The disadvantage may be that a relatively large medium length (meter scale) is required to obtain large SBS backscattering. Fortunately, optical fibers can provide a large SBS interaction length within a small volume to achieve excellent NOL performance. This proposed technology exhibits excellent NOL performance in a wide wavelength range, high laser induced damage threshold, and fast response speed, which may have important application prospects in the field of infrared broadband laser protection.

## Acknowledgement

This work was supported by the National Natural Science Foundation of China (NSFC) (Nos. 62175105 and 61875086).

## References

1. L. W. Tutt and T. F. Boggess, "A review of optical limiting mechanisms and devices using organics, fullerenes, semiconductors and other materials," *Prog. Quantum Electron.* **17**, 299 (1993).
2. J. Huang, N. Dong, S. Zhang, Z. Sun, W. Zhang, and J. Wang, "Nonlinear absorption induced transparency and optical limiting of black phosphorus nanosheets," *ACS Photonics* **4**, 3063 (2017).

**Table 1.** Comparison of Different Infrared Broadband NOL Technologies.

Materials	Limiting Principle	[ $T_{max}$ , $T_{min}$ ] [at wavelength]	Limiting Threshold [MW/cm <sup>2</sup> ]	Laser Induced Damage Threshold [GW/cm <sup>2</sup> ]	Wavelength Range
1 m As <sub>2</sub> Se <sub>3</sub> fiber [this Letter]	SBS	[90.36%, 0.89%][@3.6 μm]	22.7	>13	3–8 μm
0.5 m As <sub>2</sub> Se <sub>3</sub> fiber [this Letter]	SBS	[95.06%, 1.23%][@3.6 μm]	28.4	>13	3–8 μm
GO in NMP <sup>[10]</sup>	RSA	[81%, 42%][@1750 nm]	62.5	–	400–1800 nm
GO Ormosil glasses <sup>[32]</sup>	NA	[40%, 18%][@532 nm]	22.5	>1	532–1570 nm
GST phase change material <sup>[12]</sup>	Phase change	[80%, 0.02%][@1500 nm]	–	–	1250–2000 nm

3. O. Muller, V. Pichot, L. Merlat, and D. Spitzer, "Optical limiting properties of surface functionalized nanodiamonds probed by the Z-scan method," *Sci. Rep.* **9**, 519 (2019).
4. E. Sani, N. Papi, L. Mercatelli, S. Barison, F. Agresti, S. Rossi, and A. Dell'Oro, "Optical limiting of carbon nanohorn-based aqueous nanofluids: a systematic study," *Nanomaterials* **10**, 2160 (2020).
5. R. R. Gattass and E. Mazur, "Femtosecond laser micromachining in transparent materials," *Nat. Photonics* **2**, 219 (2008).
6. R. W. Waynant, I. K. Iiev, and I. Gannot, "Mid-infrared laser applications in medicine and biology," *Phil. Trans. R. Soc. Lond. A* **359**, 635 (2001).
7. B. M. Walsh, H. R. Lee, and N. P. Barnes, "Mid infrared lasers for remote sensing applications," *J. Lumi.* **169**, 400 (2016).
8. M. Vainio and J. Karhu, "Fully stabilized mid-infrared frequency comb for high-precision molecular spectroscopy," *Opt. Express* **25**, 4190 (2017).
9. L. G. Hølemen and M. W. Haakestad, "Optical limiting properties of carbon disulfide at 2.05  $\mu\text{m}$  wavelength," *Proc. SPIE* **9731**, 97310J (2016).
10. N. Liaros, E. Koudoumas, and S. Couris, "Broadband near infrared optical power limiting of few layered graphene oxides," *Appl. Phys. Lett.* **104**, 191112 (2014).
11. S. Pascal, S. David, C. Andraud, and O. Maury, "Near-infrared dyes for two-photon absorption in the short-wavelength infrared: strategies towards optical power limiting," *Chem. Soc. Rev.* **50**, 6613 (2021).
12. A. Sarangan, J. Duran, V. Vasilyev, N. Limberopoulos, I. Vitebskiy, and I. Anisimov, "Broadband reflective optical limiter using GST phase change material," *IEEE Photonics J.* **10**, 2200409 (2018).
13. S. Aithal, P. S. Aithal, and G. K. Bhat, "Characteristics of ideal optical limiter and realization scenarios using nonlinear organic materials," *Int. J. Adv. Trends Eng. Technol* **1**, 73 (2017).
14. L. R. Robichaud, V. Fortin, J. C. Cauthier, S. Chatigny, J. F. Couillard, J. L. Delarosbil, R. Vallee, and M. Bernier, "Compact 3–8  $\mu\text{m}$  supercontinuum generation in a low-loss  $\text{As}_2\text{Se}_3$  step-index fiber," *Opt. Lett.* **41**, 4605 (2016).
15. Y. Lv, L. Wu, and X. Chong, "Nonlinear optical properties of stimulated Brillouin scattering process in submerged object detection," *Chin. Opt. Lett.* **6**, 137 (2008).
16. J. H. Vella, J. H. Goldsmith, A. T. Browning, N. I. Limberopoulos, I. Vitebskiy, E. Makri, and T. Kottos, "Experimental realization of a reflective optical limiter," *Phys. Rev. Appl.* **5**, 064010 (2016).
17. E. P. Ippen and R. H. Stolen, "Stimulated Brillouin scattering in optical fibers," *Appl. Phys. Lett.* **21**, 539 (1972).
18. K. Kawanishi, F. Drouet, K. Itoh, and T. Konishi, "Highly accurate compensation technique for 10-GHz pulse intensity fluctuation using SPM-based all-optical intensity limiter," *IEEE Photonic Tech. Lett.* **24**, 119 (2012).
19. I. Martincsek and D. Pudis, "Fiber-optical power limiter and cut-off switch based on thermo-optical effect," *IEEE Photonic Tech. Lett.* **24**, 297 (2012).
20. X. Chen, L. Xia, W. Li, and C. Li, "Simulation of Brillouin gain properties in a double-clad  $\text{As}_2\text{Se}_3$  chalcogenide photonic crystal fiber," *Chin. Opt. Lett.* **15**, 042901 (2017).
21. A. L. Gaeta and R. W. Boyd, "Stochastic dynamics of stimulated Brillouin scattering in an optical fiber," *Phys. Rev. A* **44**, 3205 (1991).
22. R. W. Boyd, *Nonlinear Optics*, 3rd ed. (Elsevier, 2008).
23. G. P. Agrawal, *Nonlinear Fiber Optics*, 5th ed. (Elsevier, 2012).
24. W. Gao, L. Chen, W. Jiang, Z. Zhang, X. Zhang, P. Gao, K. Xie, W. Zhang, Y. Zhou, M. Liao, T. Suzuki, and Y. Ohishi, "Stimulated Brillouin scattering by the interaction between different-order optical and acoustical modes in an  $\text{As}_2\text{Se}_3$  photonic crystal fiber," *Chin. Opt. Lett.* **18**, 010602 (2020).
25. M. Zhang, L. Li, T. Li, F. Wang, K. Tian, H. Tao, X. Feng, A. Yang, and Z. Yang, "Mid-infrared supercontinuum generation in chalcogenide fibers with high laser damage threshold," *Opt. Express* **27**, 29287 (2019).
26. G. Xing, J. Jiang, J. Y. Ying, and W. Ji, " $\text{Fe}_3\text{O}_4$ -Ag nanocomposites for optical limiting: broad temporal response and low threshold," *Opt. Express* **18**, 6183 (2010).
27. E. W. V. Stryland, M. A. Woodall, H. Vanherzeele, and M. J. Soileau, "Energy band-gap dependence of two-photon absorption," *Opt. Lett.* **10**, 490 (1985).
28. K. S. Abedin, "Observation of strong stimulated Brillouin scattering in single-mode  $\text{As}_2\text{Se}_3$  chalcogenide fiber," *Opt. Express* **13**, 10266 (2005).
29. C. Florea, "Stimulated Brillouin scattering in single-mode  $\text{As}_2\text{S}_3$  and  $\text{As}_2\text{Se}_3$  chalcogenide fiber," *Opt. Express* **14**, 12063 (2006).
30. H. Gong, Z. Lv, D. Lin, and S. Liu, "Influence of medium parameters on power limiting characteristic in stimulated Brillouin scattering process," *Chin. Opt. Lett.* **5**, 674 (2007).
31. K. Ogusu, H. Li, and M. Kitao, "Brillouin-gain coefficients of chalcogenide glasses," *J. Opt. Soc. Am. B* **21**, 1302 (2004).
32. X. Sun, X. Hu, J. Sun, Z. Xie, S. Zhou, and P. Chen, "Broadband optical limiting and nonlinear optical graphene oxide co-polymerization Ormosil glasses," *Adv. Compos. Hybrid Mater.* **1**, 397 (2018).